

Development and application of novel technique for characterising the cure shrinkage of epoxy resins

Ross F. Minty¹, James L. Thomason¹, Liu Yang¹, Walter Stanley² and Ananda Roy²

¹University of Strathclyde, Department of Mechanical and Aerospace Engineering

²University of Limerick, Faculty of Science and Engineering

Ross F. Minty¹, James L. Thomason¹, Liu Yang¹, Walter Stanley² and Ananda Roy²

¹University of Strathclyde, Department of Mechanical and Aerospace Engineering, 75 Montrose Street, Glasgow G1 1XJ, United Kingdom.

²University of Limerick, Irish Composites Centre (IComp), Bernal Institute, Faculty of Science and Engineering, Castletroy, Limerick, V94 T9PX, Ireland.

Abstract

The development of a novel hot-stage microscopy technique to measure the level of cure shrinkage that occurs in an epoxy thermoset microdroplet with different epoxy-to-hardener ratios is presented. The equipment setup, sample preparation, and experimental procedure are described in detail. A comparable method to characterise cure shrinkage, a modified rheometry technique, is also reviewed. Shrinkage measurements using the hot-stage microscopy method are shown to characterise the full range of shrinkage that occurs both before and after the resin gel point, hence producing values greater than those found previously in the literature. However, when used in conjunction with the gel point values for the different ratios, measured using rheometry, the technique produces results for shrinkage post-gelation that concur well with literature values. The modified rheometry technique showed potential for measuring the level of cure shrinkage with a varying cure temperature profile, with more work required to perfect the method in defining the cross-over point for sample loading for different epoxy-to-hardener ratios.

Keywords: Chemical Shrinkage, Cure Behaviour, Thermosetting resins, Hot-stage Microscopy, Rheometry, Matrix Stoichiometry.

1. Introduction

Over the past decades it has become increasingly clear that in order to continue optimising performance of composite materials it is necessary to better measure and understand the micro-mechanical parameters that control their structure-property relationships. Composite properties result from a combination of the material properties of the fibre and the matrix as well as the capability of the fibre-matrix interface to transfer stresses. Although tailoring the interfacial stress transfer capability is widely recognised as being vital to optimising the performance of the final composite, it is routinely reduced to a discussion about improving the ‘adhesion’ between the fibre and the matrix. Adhesion represents a simplified term for encompassing the multiple complex mechanisms that exist at the interface and contribute to its strength [1–5].

Discussions about the interface in composites typically focus on the chemistry of the matrix system and the fibre surface, and the necessity to maximise the level of chemical bonding in order to optimise the level of ‘adhesion’ between the two [1,4,6–9].

However a number of authors have also commented on the role that shrinkage stresses have in influencing the stress transfer capability of the interface [10–16]. Specifically, that residual radial compressive stresses formed at the interface may be a significant contributor to the measured strength of the interface. Thermal compressive radial stresses form during the cooling process due to differences in the thermal expansion coefficients of the matrix polymer and the reinforcement fibre. However, most thermosetting matrices also undergo additional volume change during polymerisation known as cure shrinkage. Due to the increase of the glass transition temperature (T_g) as thermoset matrix reacts and shrinks it is possible for some level of this cure shrinkage to be ‘frozen’ into the system, creating additional residual stresses at the interface. It has

been shown that the contribution made by chemical cure shrinkage to the residual stresses at the interface may be greater than that of thermal shrinkage [17].

Many investigations have been conducted into evaluating potential techniques to measure the level of cure shrinkage and also how it may be influenced by variables such as curing temperature [18–24]. There is a consensus that a modified rheometry method is applicable for studying the level of cure shrinkage at different isothermal temperatures. Alternatively, the use of a gas pycnometer or the gravimetric method have been shown to be equally viable for studying cure shrinkage. In relation to the role of variables in defining shrinkage, it has been shown that an increase in curing temperature would cause the shrinkage to occur earlier and, overall, to reach a larger value [19]. The effect of different hardener ratios on the level of shrinkage and modulus development for an epoxy resin has also been studied with it also having been found that the level of cure shrinkage increases as more hardener is added to an epoxy system [21].

Outside of the limited number of studies discussed above, little in-depth work has been reported on the role of the epoxy-to-hardener ratio in defining the level of cure shrinkage that occurs during a curing process with a varying temperature profile. Studies looking at the effect of the curing temperature typically focus on isothermal temperatures or a constant heat ramp, with samples typically studied at the stoichiometric ratio. The importance of the epoxy-to-hardener ratio has been shown previously using the microbond technique to study the influence of the ratio over the interfacial shear strength (IFSS) value [25]. From the key findings, it was hypothesised that the contributions of the cure and thermal shrinkage could be influenced by the ratio

due to changes in the material properties of the cured resin. This would correlate with the IFSS values measured across different epoxy-to-hardener ratios.

Reflecting on the clear effect that matrix stoichiometry has been shown to have on the material properties of the cured resin, IFSS values measured [25] and the results discussed by Hoa et al. [21], it was deemed necessary to study how the shrinkage would occur for an epoxy microdroplet sample. It was observed that such a study has never been carried out, with the typical techniques used for studying shrinkage requiring significantly more matrix material than would be found in a microbond sample.

The present work is aimed at giving details of the development of a hot-stage microscopy technique that allowed for the measurement of cure shrinkage of an epoxy microdroplet microbond sample within the laboratory during the curing process. It covers the necessary equipment, sample preparation and analysis of readings recorded. In addition, details are provided for a modified rheometry technique that was used to compare shrinkage values over the same temperature schedule. This technique is based upon those previously reported on in the literature, however with a varying temperature schedule to match that used for the hot-stage study. The application of these techniques is demonstrated by characterising the normalised volumetric shrinkage of the epoxy matrix during polymerisation [26].

2. Methodology

2.1 Materials

Single boron free E-glass fibres, coated with γ -aminopropyltriethoxysilane (APS) were taken from larger rovings supplied by Owens Corning-Vetrotex. The nominal tex was 1200 g/km and the average diameter was 17.5 μm . Araldite[®] 506 epoxy resin and

triethylenetetramine (TETA) curing agent were purchased from Sigma-Aldrich and used as received. The stoichiometric ratio for the system was calculated as 12% TETA and samples were prepared over a range of ratios from 7% TETA up to 22% TETA in increments of 2.5% for the hot-stage technique. Due to time constraints only the ratios of 7%, 12% and 22% were investigated using the modified rheometry technique. This equated to an amine group: epoxy group ratio (R) varying from approximately 0.5 to 2.0 for both methods studied.

2.2 Hot-stage Microscopy Technique

During analysis of past literature, it was discovered that no technique had been previously developed for studying microbond samples during the curing process to gauge the level of shrinkage that occurs. As such it was challenging to apply the findings in literature to micro-scale samples without investigating whether scaling would be an issue. This led to the development of a new method using a Mettler Toledo FP90 hot-stage heating element combined with a microscope and camera. The hot-stage setup allowed for a controlled temperature schedule to be programmed to match the cure schedule used in the preparation of microbond samples previously [11,25].

Samples were prepared by suspending single glass fibres, taken from larger bundles of E-glass fibres coated with APS, above 1 mm thick rectangular glass slide cover slips using a slow setting cement (see Figures 1 and 2). This fibre sample was then left for 24 hours to allow the cement to set. The procedure was extremely delicate due to a number of variables that had to be carefully regulated. Firstly, the glass fibre could not be allowed to touch the surface of the cover slip in case of contamination. Secondly, it had to be ensured that the fibre was suspended as straight as possible relative to the cover

slip to allow for easier analysis under the microscope. Finally, the height of cement used had to be carefully controlled to prevent it from coming in contact with the inside of the hot-stage heating element during the experiment.

Once the fibres had been successfully suspended, a minute droplet of epoxy was applied using a thin piece of steel wire with a schematic of a typical sample shown in Figure 1. Photos of a completed sample are provided in Figure 2 with the position of the microdroplets marked. The sample was then placed in the hot-stage, ready for the curing process to start, in as short a time as possible. Seven different ratios were studied with at least five samples tested per ratio. The temperature schedule selected for the test followed a similar curing schedule to that used in a microbond study of glass-epoxy adhesion [25], as shown in Figure 3.

An Olympus BX51 microscope (200x magnification) was used to allow to monitor any dimensional changes of the minute epoxy resin droplets. Images of samples were taken at one-minute intervals over the duration of the cure using a Nikon Coolpix P5100 digital camera, mounted to the head of the microscope as shown in Figure 4. It was found that, if left unchecked, the focus of the microscope could drift during the curing process and as such the user was required to be present throughout the test to ensure that this was minimised.

Once the curing process had completed the images collected were analysed for each sample using the image processing software package ImageJ, an open source, freely available software package that allows for the distance within images to be measured. Calibration of the software was of key importance to ensure that all images were analysed to a consistent scale, hence why it was required that the user ensure that the

level of magnification was maintained as close to constant as possible whilst the test was conducted. For each image the distances “a” and “b”, as shown in Figure 5, were measured and recorded.

The distance “a” was selected to be the minor axis and “b” the major axis. To allow for the volume of the droplet at each interval to be calculated several assumptions had to be made. First, it was assumed that the resin droplet remained symmetrical throughout the curing process, with any droplets developing deformities removed from the final result for each ratio. Typically, to calculate the volume of a spheroid three dimensions are required however since only two were known (dimensions a and b) it was assumed that the ideal model for the minute resin droplets embedded on the fibre was an ellipsoid. The initial size of each droplet was difficult to prepare at a constant value thus the distances were normalised to the initial dimensions to give an overall percentage change. The volume of each droplet (V_D) was calculated using Equation 1.

$$V_D = \frac{4}{3}\pi \left(\frac{a}{2}\right)^2 \left(\frac{b}{2}\right) \quad (1)$$

The normalised volumetric shrinkage (ε_V) was then calculated using:

$$\varepsilon_V = \frac{V_t - V_o}{V_o} \quad (2)$$

Where V_o represents the initial volume of the sample whilst V_t represents the volume of the sample after time t during the curing process [26].

2.3 Modified Rheometry Technique

This technique was based on the modification of the rheometry methods used by Shah et al. [18] and Khoun et al. [19] to study cure shrinkage. It focused on the measurement of the gap variation between the parallel plates of a rheometer (HR-2 Discovery Hybrid

Rheometer (DHR) from TA Instruments) as a sample of epoxy was cured. A controlled normal force was applied to maintain the contact between the two plates and the resin sample with the schematic of the setup shown in Figure 6. Ultimately the goal was to first measure the gel point and then the level of cure shrinkage (after gelation). These parameters were then studied over a range of epoxy systems from the stoichiometric value to systems possessing excess epoxy and hardener respectively. Three ratios were studied with three samples measured for the gel point and a further three samples for investigating the level of shrinkage, for two of the three ratios. Due to time constraints, only two samples were studied for the $R \approx 2.0$ ratio.

Unlike the hot-stage technique, the modified rheometry technique required the sample to have gelled before accurate measurements could be taken. This was due to the possibility of the sample resin being pushed out from between the plates if a normal force was applied to the liquid resin. As such the procedure was split into two stages:

- i. Pre-gelation;
- ii. Post-gelation;

The resin was prepared and mixed as previously and then applied to the disposable 25 mm bottom plate of the rheometer. The plate included a drip channel to account for any spillage. Pre-gelation involved the sample undergoing a single-frequency stress-controlled test conducted at a frequency of 0.2 Hz in oscillation mode with the gap between plates being maintained at 0.5 mm and the strain at 15%, with no normal force applied. The sample was then exposed to the same thermal schedule used for the hot-stage technique. This is where the technique differs from that of Shah [18] or Khoun [19] which maintained an isothermal temperature throughout.

Two options were available for defining when gelation had occurred, with the first being the cross-over point of the elastic modulus G' and viscous modulus G'' . Although this represented a viable method, it required more user input in order to ensure the correct point had occurred before switching over to step two. Alternatively, the value of 500 Pa s for viscosity has also been used in literature [19] to define the point when the second stage was initiated. Based on this finding, it was this latter procedure that was used in the cure shrinkage tests conducted in this study.

Once gelation had occurred the procedure moved to the second stage, which involved a single frequency stress-controlled test being conducted at 30 Hz in oscillation mode. This required a torque of 500 μNm and compressive force of 0.1 N to be applied under isothermal conditions. The gap between the plates then began to vary due to shrinkage, allowing for it to be recorded by the rheometer. This change would then be used with Equation 3 to define the level of cure shrinkage.

$$\varepsilon_V = \left[1 + \frac{1}{3} \left(\frac{h - h_0}{h_0} \right) \right]^3 - 1 \quad (3)$$

3. Results and discussion

3.1 Hot-stage Microscopy Technique

Figure 7 plots the normalised dimension reduction for the dimensions a and b of a droplet with a ratio of $R \approx 1.0$. It can be seen that the main portion of the cure shrinkage measured occurs during the initial heat ramp up to 60 °C and then the isotherm that occurs afterwards. By the time of the second heat ramp up to 120 °C it appears that no further cure shrinkage occurs.

Figure 8 further highlights that most of the cure shrinkage occurs early on during the curing process before then reaching a relatively constant value. Specifically, it can be seen that after about 50 minutes, virtually all the cure shrinkage had occurred for the $R \approx 1.0$ samples. This represented a point where the sample was in the 60 °C isothermal cure stage. This means that the further isothermal at 120 °C appears to cause no significant shrinkage of the microdroplet samples relative to the initial phases.

Following this initial analysis, the final isothermal was removed for the bulk of the testing to allow for the test to be carried out in a shorter time period with no apparent loss of data.

Figure 9 shows the results recorded for the $R \approx 1.0$ samples exposed to the modified cure schedule. The initial measured diameters of the droplets are listed for reference. It can be seen in Figure 9 that a good degree of correlation has been achieved between the five different tests, with the main portion of shrinkage occurring during the first 20 minutes. This takes place during the initial heat ramp up to 60 °C despite the expected thermal expansion that occurs due to the heating process of the droplet. The level of shrinkage that occurs is shown to be independent of the initial droplet diameter, with the 48.6 μm droplet shown to experience comparable shrinkage to droplets where the diameter $> 75 \mu\text{m}$. This is a positive sign since it implies that the test is not impeded by varying droplet dimensions, a variable which is typically very difficult to control when preparing microbond samples.

By taking the average of the different plots shown in Figure 9, along with those for the other ratios a comparison plot can be constructed as shown in Figure 10. The corresponding temperature during the curing process is also plotted. The data from

Figure 10 were also used to construct Figure 11 to show the influence of the R value over the level of shrinkage more distinctly.

Overall the plots show that as the R value of the matrix system was increased the corresponding level of shrinkage also increased, agreeing with the findings of Hoa [21] despite the different methods used. The overall difference is shown to be of significant size, with the smallest shrinkage value measured as $\approx 13\%$ for $R \approx 0.5$ whilst the largest is $\approx 26\%$ for $R \approx 2.0$ in Figure 10. As with Figure 9, it appears that the greatest amount of shrinkage occurs during the initial heat ramp up to $60\text{ }^\circ\text{C}$, with the second ramp up to $120\text{ }^\circ\text{C}$ seemingly not having any significant affect.

However, the values measured using the hot-stage technique appear significantly larger than those reported in the literature [18,19,23,24,27] obtained using other techniques. It is observed that one general difference between the hot-stage microdroplet method and other cure shrinkage techniques is that the hot-stage allows for measurement as soon as the curing process begins. Other techniques such as those based on thermomechanical analysis (TMA) or rheometry are reliant on the polymer having gelled before being able to measure any further shrinkage. This distinction is important, since any cure shrinkage measured prior to the gel point would result in residual stresses formed at the fibre-matrix interface that would relax away to some degree. These stresses would not contribute significantly to the stress transfer capability of the interface. Hence, although the values shown in Figure 10 are larger than expected, potentially a great degree of the residual stresses formed by this cure shrinkage will have relaxed away. For a true representation of the data to be shown the gel point of each R value would need to be

known and then applied; this conclusion resulted in the study of the gel point using rheometry [26].

3.2 Rheometry – Gel Point Investigation

With the completion of the hot-stage microscopy study it became clear that more information regarding the gel point of the epoxy system was required if the results from the hot-stage technique were to be compared with other accepted methods for measuring cure shrinkage. Specifically, whether the gel point would be influenced by the R value and at what point in time each mixture would gel during the cure schedule shown in Figure 3. This information would allow for the level of cure shrinkage after gelation to be established and the results from the hot-stage method to then be compared to the other techniques discussed in the literature.

The primary technique used to define the gel point during these tests was the cross-over point of G' and G'' as shown in Figure 12 with the results presented in Table 1.

Table 1. Average gel point values according to moduli crossover point.

Ratio	$R \approx 0.5$	$R \approx 1.0$	$R \approx 2.0$
Average Gel Point (s)	3060	2252	1982
Standard Deviation	157	37	108
95% Confidence	178	42	150

Another technique for calculating the gel point involves extrapolating the viscosity data for each sample and determining the time at which the viscosity began to increase exponentially. An example of such a plot is provided in Figure 13 with the data obtained shown in Table 2. Comparing the two sets of data in Tables 1 and 2, it can be seen that the values correlate well with each other.

Table 2. Average gel point values according to viscosity extrapolation.

Ratio	R \approx 0.5	R \approx 1.0	R \approx 2.0
Average Gel Point (s)	3313	2306	2018
Standard Deviation	121	13	126
95% Confidence	137	14	174

Overall it can be seen that the R value did have a considerable influence over the gel point of the system as shown in Figure 14. As the R value was increased the gel point of the matrix system was shown to decrease, with R \approx 2.0 found to gel after \approx 33 minutes. This compares to \approx 51 minutes for R \approx 0.5, highlighting the significant difference between the two extreme values. The difference between R \approx 0.5 and R \approx 1.0 appears notably larger than that shown between R \approx 1.0 and R \approx 2.0. This phenomenon implies that adding extra amine groups to the reacting system will lead to the reaction speeding up, and thus would influence the level of shrinkage measured using the hot-stage technique.

Interestingly for each of the ratios the gel point was shown to occur during the 60 °C isothermal stage of the curing process shown in Figure 3. According to Figure 10 this would suggest that a large degree of the initial shrinkage induced stresses would not be frozen into the system and instead will have relaxed away. Thus, the hypothesis that the actual degree of residual stress that will be frozen into the network will be smaller than that implied by the shrinkage levels seen in Figure 10 was shown to be correct.

Applying the gel point data to the hot-stage microscopy data creates the plot shown in Figure 15, which shows the actual level of cure shrinkage that could result in stresses being frozen into the system during the curing process. It can be seen that the cure shrinkage values shown in Figure 15 are notably smaller than those initially shown in

Figure 8, with the values measured now varying between 2% up to 7% depending on the R value. These values now correlate well with those discussed in published literature [17–19,21,24,28], suggesting that the hot-stage microscopy technique is indeed a viable method for studying cure shrinkage [26].

3.3 Modified Rheometry Technique

To provide a direct comparison, a modified rheometry technique was used to study the cure shrinkage of different R values exposed to the curing schedule shown in Figure 3. A key aspect of this technique was setting the point at which the technique would transition from the pre-gelation phase to the post-gelation phase, where the cure shrinkage would be measured. The value of 500 Pa s had been used previously in the literature [19] and was deemed acceptable for use with the Araldite® 506 - TETA system. However, the transition point of 500 Pa s was found to be inconsistent when defining a clear gel point for the different R values. As a result, it was found that some samples could undergo a large degree of compression, with some resin being pushed out from between the plates, due to it having not sufficiently gelled before loading was applied. This can clearly be seen in Figure 16 where each sample initially undergoes a large decrease in the gap between the rheometer plates, before then levelling off to some degree, whereupon the actual shrinkage measurement during curing begins as shown in Figure 17. It appears that this phenomenon applies to each of the R values studied.

Although this clearly hinders the measurement of the cure shrinkage, it can be seen in the plot that shrinkage does indeed occur once the system has gelled. The samples are shown to undergo a degree of cure shrinkage of a magnitude similar to that in Figure 15. Yet unlike Figure 15 there is a notable dip downwards for each ratio where the

temperature began the second temperature ramp up to 120 °C, suggesting that shrinkage was still occurring at this point. In addition, this is followed by a slight increase in the gap width as the temperature approaches 120 °C, implying potential expansion of the sample due to the increase in rheometer temperature. It is notable that such an expansion is not present in the hot-stage data shown in Figure 10. These differences combined with the initial starting point for each sample varying greatly make it difficult to discern whether the shrinkage measured was accurate or not.

Despite the concerns considering the applicability of the technique, when the data from Figure 16 is used with Equation 3, it does produce a plot that compares favourably to the data found using the hot-stage technique. Figure 18 shows that the two data sets correlate well for two of the three ratios studied, with a distinct difference shown for $R \approx 2.0$ which was the ratio with the fewest samples studied. This would suggest that the rheometer method may not be as accurate for ratios where $R > 1.0$. An explanation for this may be due to the faster gel point of the higher ratios leading to difficulties in accurately measuring the level of shrinkage from the initial stages after the gel point. This hypothesis would be supported by the fact that the results for the other two ratios studied compare very favourably. However, due to the variation in initial gap sizes discussed, it is difficult to fully confirm whether this is the case without future experiments and analysis.

Overall it appears that the modified rheometer technique is a potentially viable method for studying cure shrinkage with a varying temperature profile. The values produced for cure shrinkage appear comparable, to a degree, with those shown for the hot-stage technique despite the difficulties encountered. The true level of shrinkage that may have

occurred was difficult to fully evaluate due to the large initial drop in the gap between rheometer plates, which varied for each sample. It was concluded that in future the viscosity value of 500 Pa s was not a viable transition point for this method, due to the changing R values combined with the varying temperature. As such, it is recommended that the user identify the point where G' and G'' cross during the experiment before then manually instructing the software to begin the loading phase. This would ensure that the material would have gelled before loading, ensuring that any further gap changes measured was due to the chemical cure shrinkage reaction. This would negate the variation that was shown between the different samples.

4. Conclusions

This paper has discussed the development of a novel technique using hot-stage microscopy which can be used to measure the cure shrinkage of a minute epoxy droplet upon a single fibre during its curing process. It was shown that as the R value of the system was increased, the level of cure shrinkage that occurred increased. Thus, the contribution to the stress transfer capability of the interface due to residual radial compressive stresses caused by this shrinkage could be influenced by the hardener-to-epoxy ratio. The values measured using the technique were found to be noticeably larger than those reported in the literature, however this was due to technique measuring all possible shrinkage that would occur. To account for this the gel point for the different ratios was required to discern how much shrinkage could be frozen into the matrix structure.

A rheometry study showed that the gel point of the matrix system was indeed influenced by the R value. As the R value was increased the gel point was shown to occur earlier.

Since the same schedule was used in the rheometer study and the hot-stage shrinkage measurements, the gel points could then be applied to the hot-stage data. Taking this into account, the post-gelation shrinkage values for $R \approx 0.5$, $R \approx 1.0$ and $R \approx 2.0$ were calculated and these appeared consistent with values reported in the literature.

A modified rheometry based technique also appeared to show potential for measuring the level of cure shrinkage with a varying temperature profile. However, more work is required to fully perfect this method due to difficulties in defining the cross-over point for sample loading. This will be subject to further research.

Acknowledgements

The authors gratefully acknowledge the support of the Engineering and Physical Sciences Research Council (EPSRC). We would also like to thank the Irish Composites Centre at the University of Limerick for access to their rheometry equipment and expertise in conducting such research.

Data Availability

The raw/processed data required to reproduce these findings cannot be shared at this time as the data also forms part of an ongoing study. The research was conducted as part of the EPSRC project “Interfacial Adhesion and Mechanical Performance in Composites for Wind Turbine Applications” (reference: 1568745).

References

- [1] R. Plonka, E. Mäder, S.L. Gao, C. Bellmann, V. Dutschk, S. Zhandarov, Adhesion of epoxy/glass fibre composites influenced by aging effects on sizings, *Compos. Part A Appl. Sci. Manuf.* 35 (2004) 1207–1216.

doi:10.1016/j.compositesa.2004.03.005.

- [2] P.J. Herrera-Franco, L.T. Drzal, Comparison of methods for the measurement of fibre/matrix adhesion in composites, *Composites*. 23 (1992) 2–27.
doi:10.1016/0010-4361(92)90282-Y.
- [3] M. Nardin, J. Schultz, Relationship between fibre-matrix adhesion and the interfacial shear strength in polymer-based composites, *Compos. Interfaces*. 1 (1993) 177–192. doi:10.1163/156855493X00068.
- [4] L.T. Drzal, M. Madhukar, Fibre-matrix adhesion and its relationship to composite mechanical properties, *J. Mater. Sci.* 28 (1993) 569–610.
doi:10.1007/BF01151234.
- [5] K. Szymczyk, A. Zdziennicka, J. Krawczyk, B. Jańczuk, Wettability, adhesion, adsorption and interface tension in the polymer/surfactant aqueous solution system: II. Work of adhesion and adsorption of surfactant at polymer-solution and solution-air interfaces, *Colloids Surfaces A Physicochem. Eng. Asp.* 402 (2012) 139–145. doi:10.1016/j.colsurfa.2012.02.055.
- [6] L.J. Broutman, Measurement of the Fiber-Polymer Matrix Interfacial Strength, *Interfaces Compos. ASTM STP 452*. (1969) 27–41.
- [7] M. Dey, J.M. Deitzel, J.W. Gillespie, S. Schweiger, Influence of sizing formulations on glass/epoxy interphase properties, *Compos. Part A Appl. Sci. Manuf.* 63 (2014) 59–67. doi:10.1016/j.compositesa.2014.04.006.
- [8] R.J. Gray, C.D. Johnston, The effect of matrix composition on fibre/matrix interfacial bond shear strength in fibre-reinforced mortar, *Cem. Concr. Res.* 14 (1984) 285–296. doi:10.1016/0008-8846(84)90116-9.
- [9] F.R. Jones, A Review of Interphase Formation and Design in Fibre-Reinforced

- Composites, 2010. doi:10.1163/016942409X12579497420609.
- [10] J.L. Thomason, L. Yang, Temperature dependence of the interfacial shear strength in glass-fibre polypropylene composites, *Compos. Sci. Technol.* 71 (2011) 1600–1605. doi:10.1016/j.compscitech.2011.07.006.
- [11] J.L. Thomason, L. Yang, Temperature dependence of the interfacial shear strength in glass-fibre epoxy composites, *Compos. Sci. Technol.* 96 (2014) 7–12. doi:10.1016/j.compscitech.2014.03.009.
- [12] J.A. Nairn, Thermoelastic analysis of residual stresses in unidirectional, high-performance composites, *Polym. Compos.* 6 (1985) 123–130. doi:10.1002/pc.750060211.
- [13] R.S. Raghava, Thermal expansion of organic and inorganic matrix composites: A Review of theoretical and experimental studies, *Polym. Compos.* 9 (1988) 1–11. doi:10.1002/pc.750090102.
- [14] H.D. Wagner, J.A. Nairn, Residual thermal stresses in three concentric transversely isotropic cylinders: application to composites containing a interphase., *Compos. Sci. Technol.* 57 (1997) 1289–1302. doi:10.1016/S0266-3538(97)00058-4.
- [15] L. Di Landro, M. Pegoraro, Carbon fibre thermoplastic matrix adhesion, *J. Mater. Sci.* 22 (1987) 1980–1986. doi:10.1007/BF01132927.
- [16] D.A. Biro, G. Pleizier, Y. Deslandes, Application of the microbond technique: Effects of hygrothermal exposure on carbon-fiber/epoxy interfaces, *Compos. Sci. Technol.* 46 (1993) 293–301. doi:10.1016/0266-3538(93)90163-B.
- [17] J. Jakobsen, M. Jensen, J.H. Andreasen, Thermo-mechanical characterisation of in-plane properties for CSM E-glass epoxy polymer composite materials – Part 1:

- Thermal and chemical strain, *Polym. Test.* 32 (2013) 1350–1357.
doi:10.1016/j.polymertesting.2013.08.010.
- [18] D.U. Shah, P.J. Schubel, Evaluation of cure shrinkage measurement techniques for thermosetting resins, *Polym. Test.* 29 (2010) 629–639.
doi:10.1016/j.polymertesting.2010.05.001.
- [19] L. Khoun, P. Hubert, Cure Shrinkage Characterization of an Epoxy Resin System by Two in Situ Measurement Methods, *Polym. Compos.* 31 (2010) 1603–1610.
doi:10.1002/pc.
- [20] Y. Nawab, S. Shahid, N. Boyard, F. Jacquemin, Chemical shrinkage characterization techniques for thermoset resins and associated composites, *J. Mater. Sci.* 48 (2013) 5387–5409. doi:10.1007/s10853-013-7333-6.
- [21] S. V. Hoa, P. Ouellette, T.D. Ngo, Determination of Shrinkage and Modulus Development of Thermosetting Resins, *J. Compos. Mater.* 43 (2009) 783–803.
doi:10.1177/0021998308102035.
- [22] J. Parameswaranpillai, A. George, J. Pionteck, S. Thomas, Investigation of Cure Reaction, Rheology, Volume Shrinkage and Thermomechanical Properties of Nano-TiO₂ Filled Epoxy/DDS Composites, *J. Polym. Sci. Part B: Polym. Phys.* 51 (2013) 1–17.
doi:10.1155/2013/183463.
- [23] K.F. Schoch, P.A. Panackal, P.P. Frank, Real-time measurement of resin shrinkage during cure, *Thermochim. Acta.* 417 (2004) 115–118.
doi:10.1016/j.tca.2003.12.027.
- [24] H. Yu, S.G. Mhaisalkar, E.H. Wong, Cure shrinkage measurement of nonconductive adhesives by means of a thermomechanical analyzer, *J. Electron. Mater.* 34 (2005) 1177–1182. doi:10.1007/s11664-005-0248-5.

- [25] R.F. Minty, L. Yang, J.L. Thomason, The influence of hardener-to-epoxy ratio on the interfacial strength in glass fibre reinforced epoxy composites, *Compos. Part A*. 112 (2018) 64–70. doi:10.1016/j.compositesa.2018.05.033.
- [26] R.F. Minty, The Influence of Matrix Stoichiometry on Interfacial Adhesion in Composites for Wind Turbine Applications, PhD Thesis, University of Strathclyde, 2018.
- [27] J.L. Thomason, L. Yang, Temperature dependence of the interfacial shear strength in glass- fibre epoxy composites., *Compos. Sci. Technol.* 96 (2014) 7–12. doi:10.1016/j.buildenv.2006.10.027.
- [28] C. Li, K. Potter, M.R. Wisnom, G. Stringer, In-situ measurement of chemical shrinkage of MY750 epoxy resin by a novel gravimetric method, *Compos. Sci. Technol.* 64 (2004) 55–64. doi:10.1016/S0266-3538(03)00199-4.

Figure Captions

Figure 1. Hot-stage microscopy sample schematic.

Figure 2. Photos of hot-stage microscopy sample with the position of the microdroplet(s) highlighted.

Figure 3. Temperature schedule of hot-stage microscopy technique.

Figure 4. Photos of hot-stage and microscope setup.

Figure 5. Photos of epoxy microdroplet under microscope showing level of cure shrinkage after 0 minutes and 20 minutes respectively. The distances a and b are highlighted. Figure 6. Schematic of rheometer cure shrinkage setup.

Figure 7. Normalised dimension reduction versus time plot for a sample with a ratio of $R \approx 1.0$ for full cure schedule.

Figure 8. Normalised volumetric reduction versus time plot for $R \approx 1.0$ samples for full cure schedule.

Figure 9. Normalised volumetric shrinkage versus time plot for $R \approx 1.0$ samples for modified cure schedule.

Figure 10. Normalised volumetric shrinkage versus time comparison plot for all R values studied.

Figure 11. Normalised volumetric shrinkage versus R value comparison plot after specific time periods.

Figure 12. Crossover point of G' and G'' used as one technique to define the gel point of the sample ($R \approx 1.0$).

Figure 13. Extrapolation of viscosity plot for gel point of sample ($R \approx 1.0$).

Figure 14. Plot of gel point versus R value.

Figure 15. Adjusted cure shrinkage results measured using hot-stage microscopy taking account for gel point.

Figure 16. Plot of rheometer plate gap width versus time into curing schedule.

Figure 17. Magnified plot of rheometer plate gap width versus time into curing schedule for sample number 2 with a R ratio of 1.0.

Figure 18. Comparison of cure shrinkage results measured using the rheometer and hot-stage techniques.

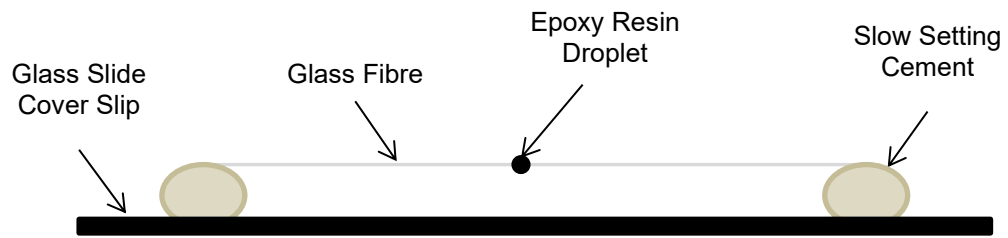


Figure 1. Hot-stage microscopy sample schematic.



Figure 2. Photos of hot-stage microscopy sample with the position of the microdroplet(s) highlighted.

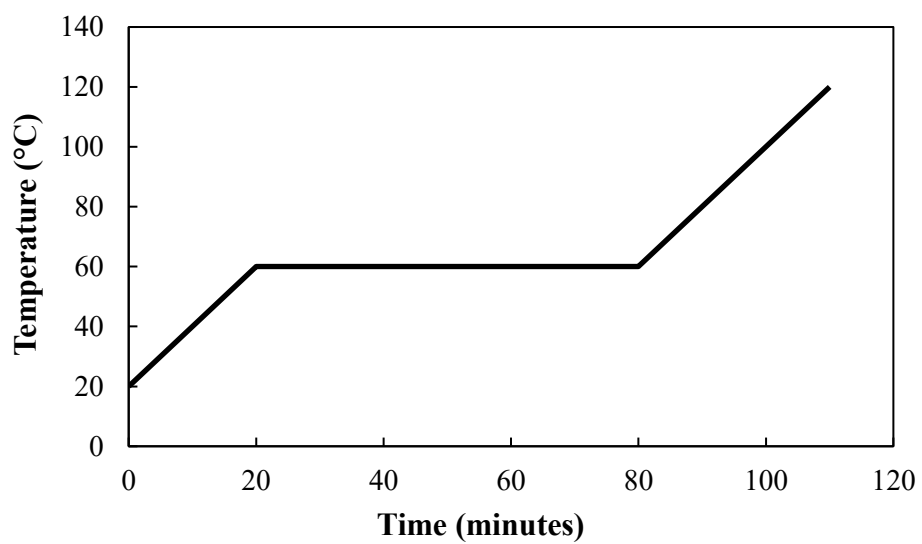


Figure 3. Temperature schedule of hot-stage microscopy technique.



Figure 4. Photos of hot-stage and microscope set-up.

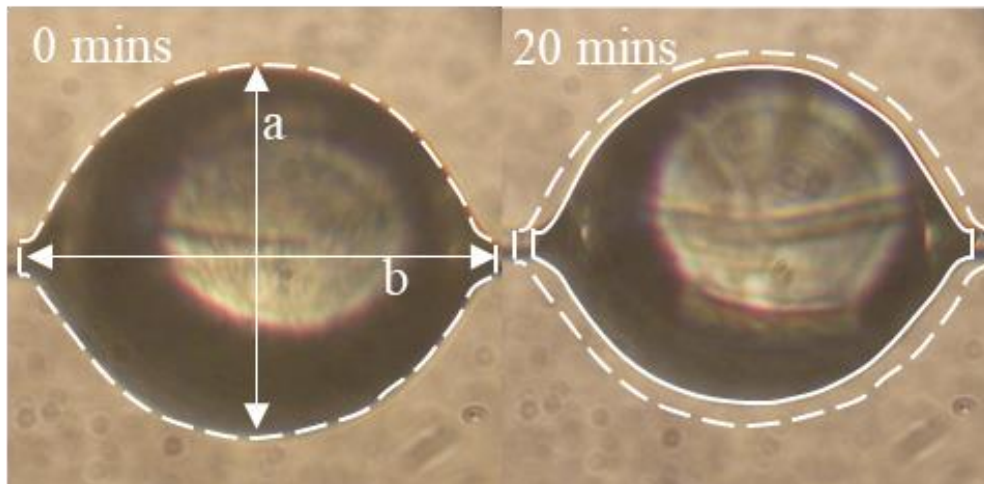


Figure 5. Photos of epoxy microdroplet under microscope showing level of cure shrinkage after 0 minutes and 20 minutes respectively. The distances a and b are highlighted.

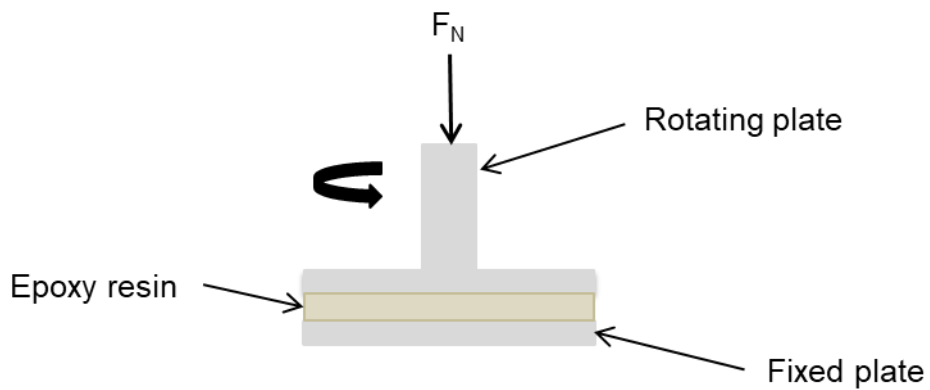


Figure 6. Schematic of rheometer cure shrinkage setup.

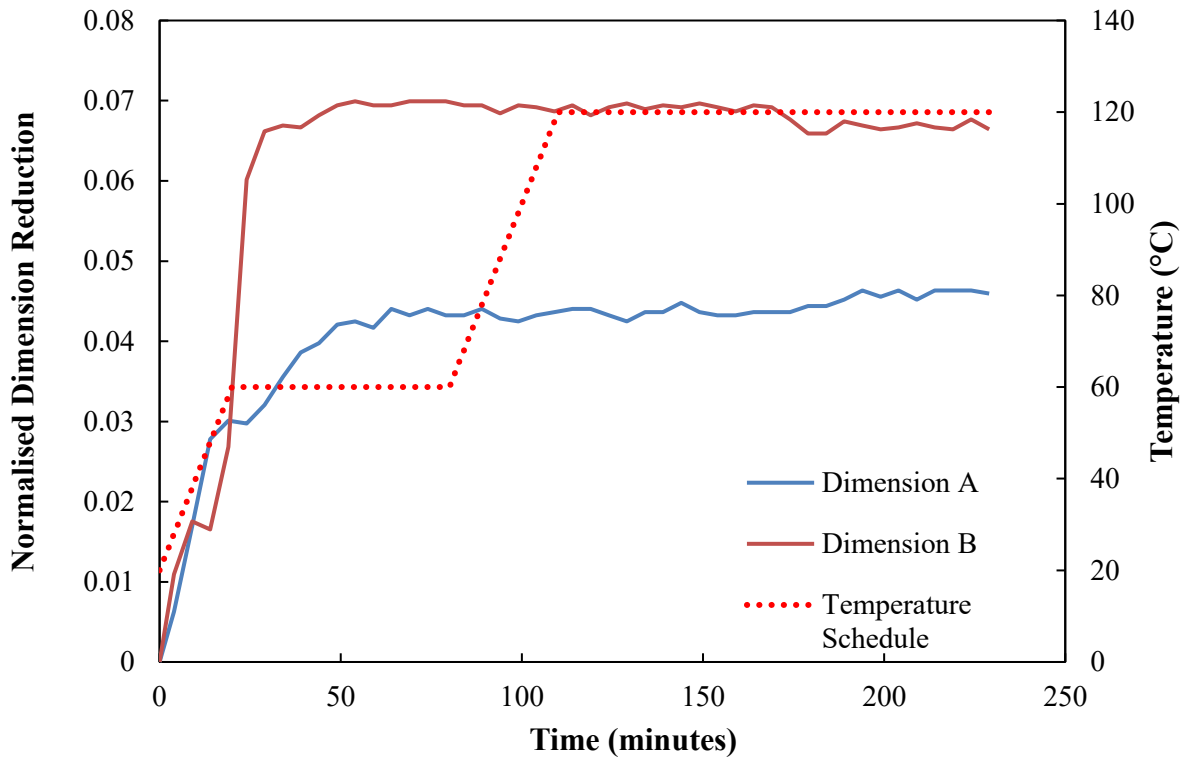


Figure 7. Normalised dimension reduction versus time plot for a sample with a ratio of $R \approx 1.0$ for full cure schedule.

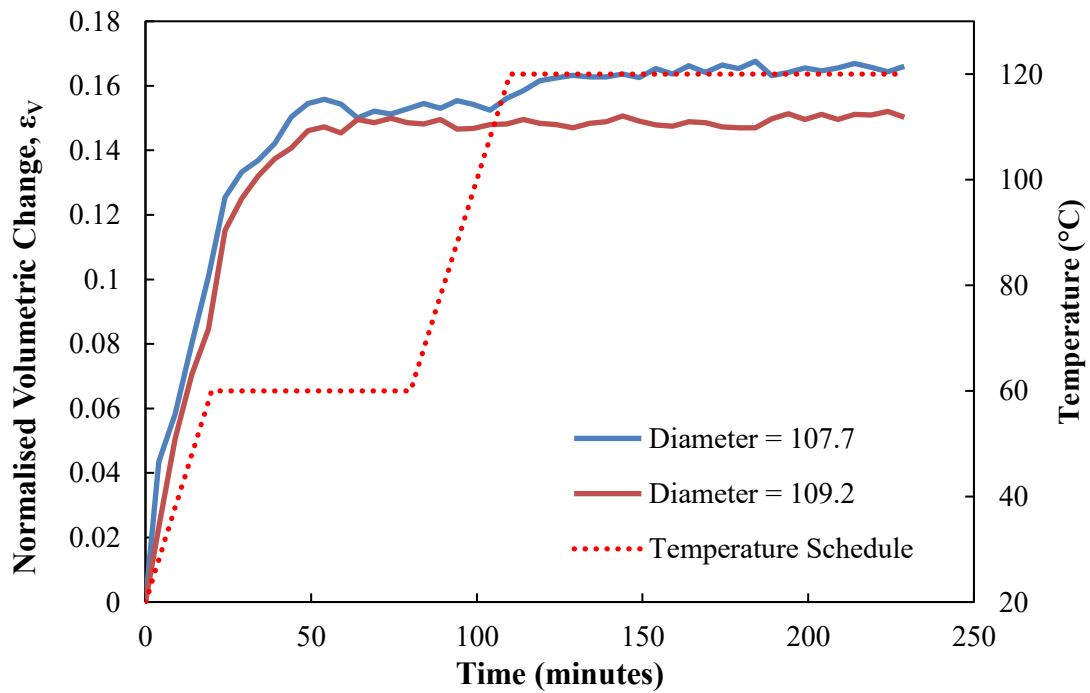


Figure 8. Normalised volumetric reduction versus time plot for $R \approx 1.0$ samples for full cure schedule.

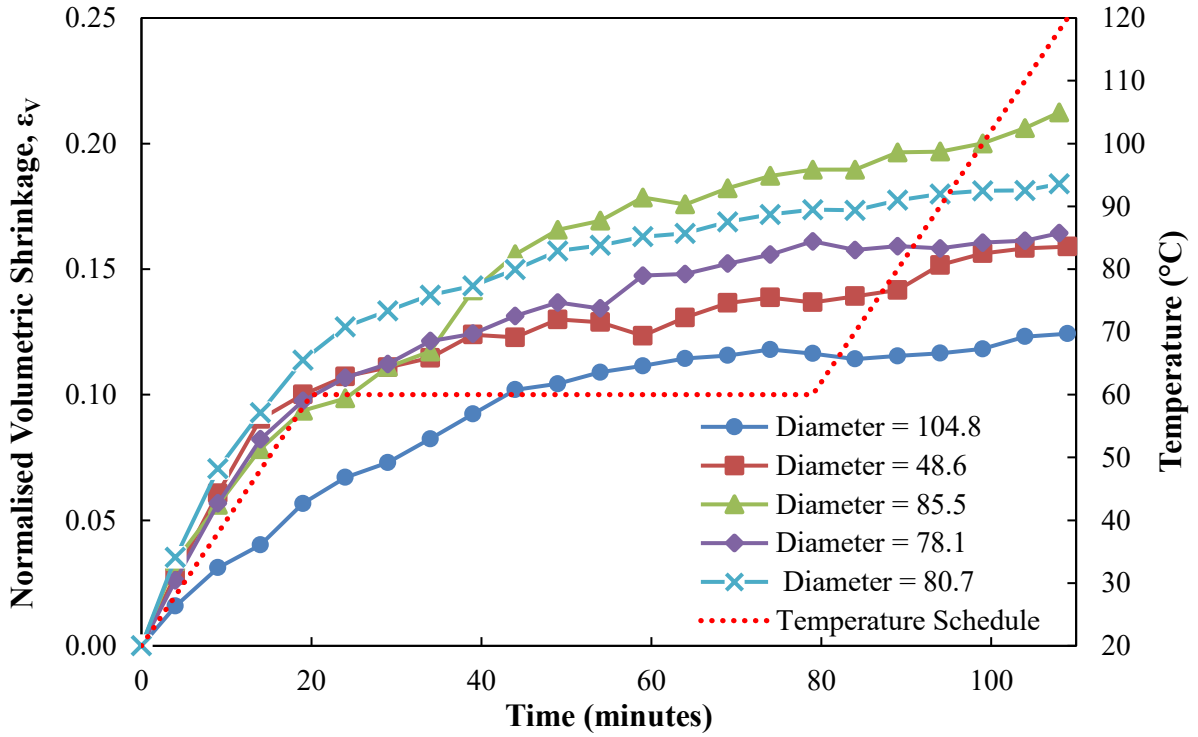


Figure 9. Normalised volumetric shrinkage versus time plot for $R \approx 1.0$ samples for modified cure schedule.

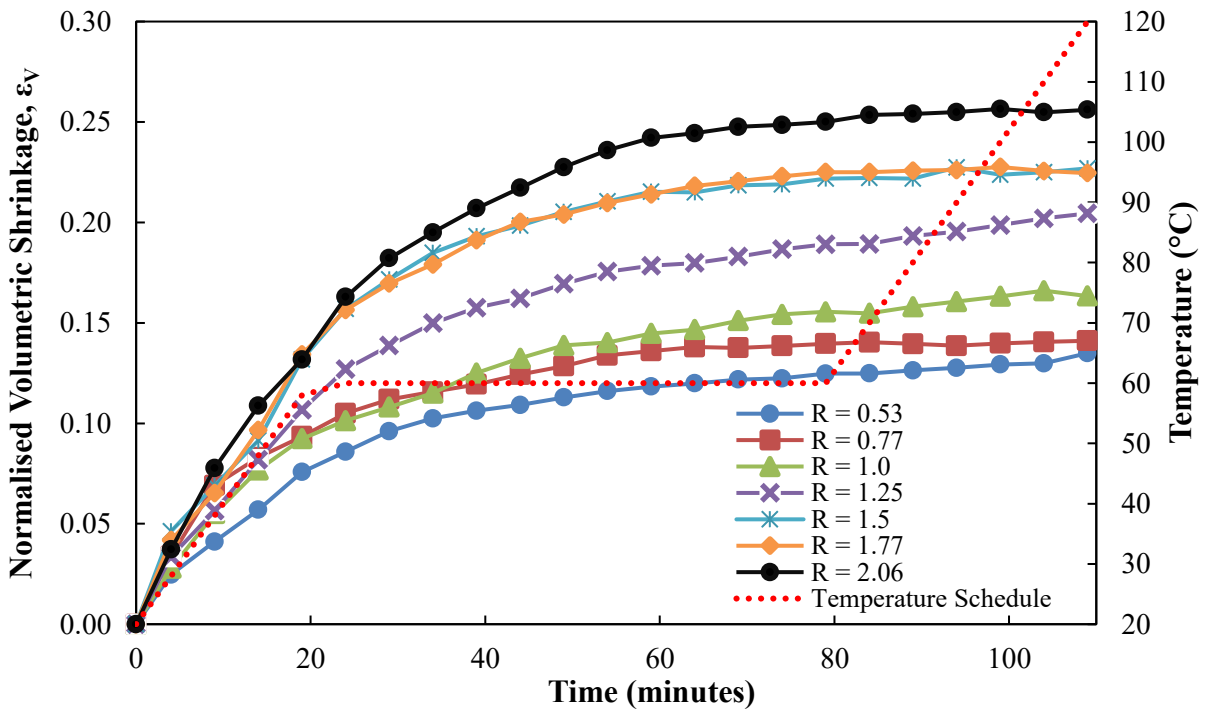


Figure 10. Normalised volumetric shrinkage versus time comparison plot for all R values studied.

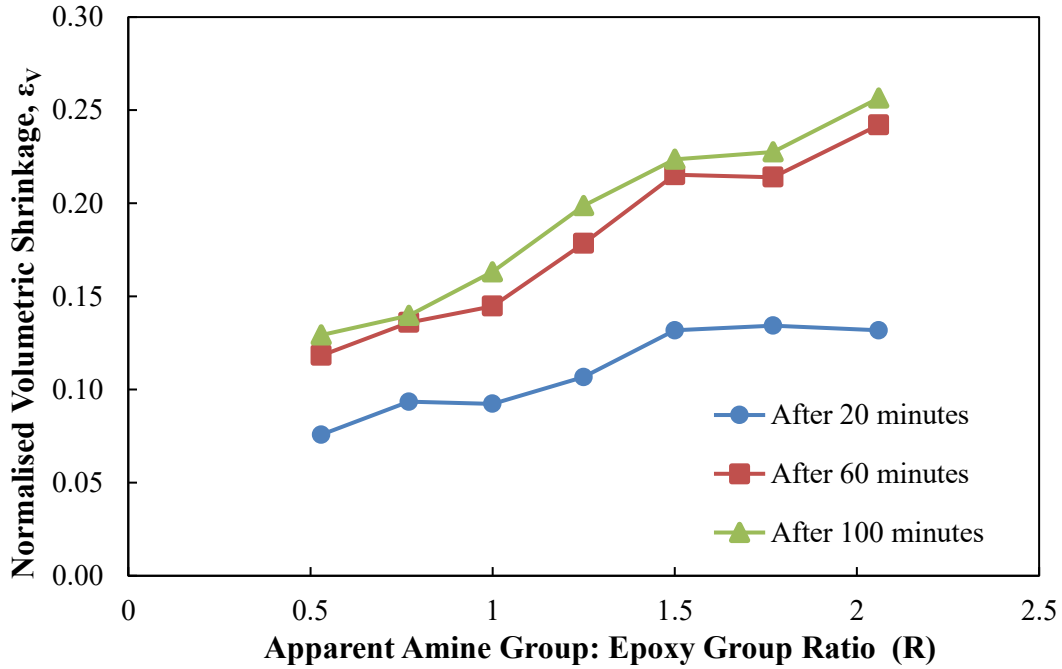


Figure 11. Normalised volumetric shrinkage versus R value comparison plot after specific time periods.

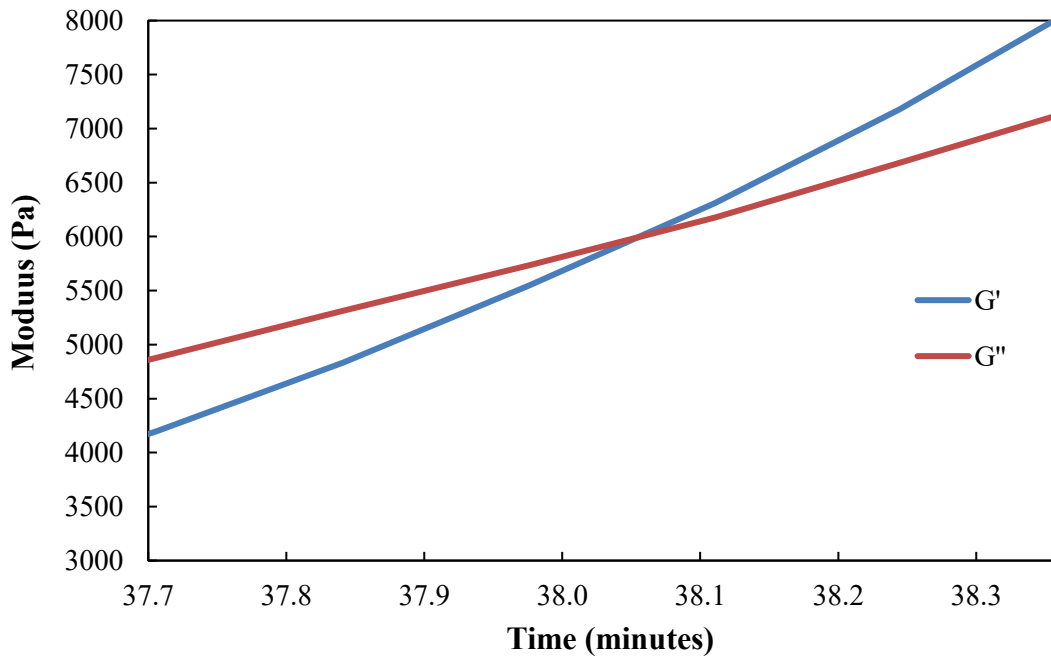


Figure 12. Crossover point of G' and G'' used as one technique to define the gel point of the sample ($R \approx 1.0$).

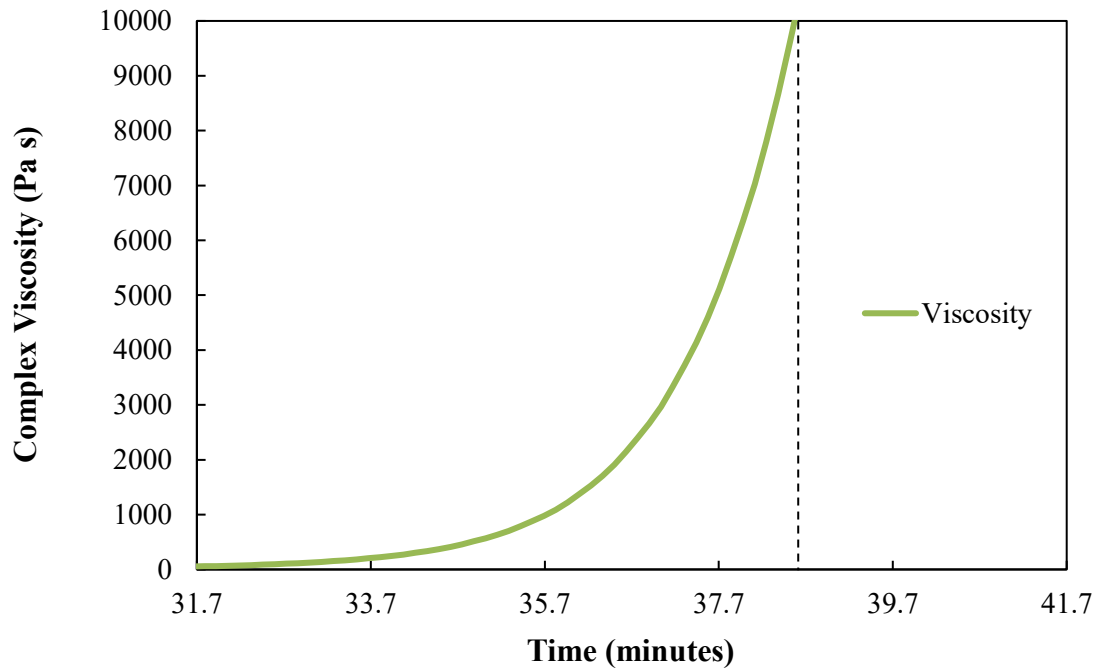


Figure 13. Extrapolation of viscosity plot for gel point of sample ($R \approx 1.0$).

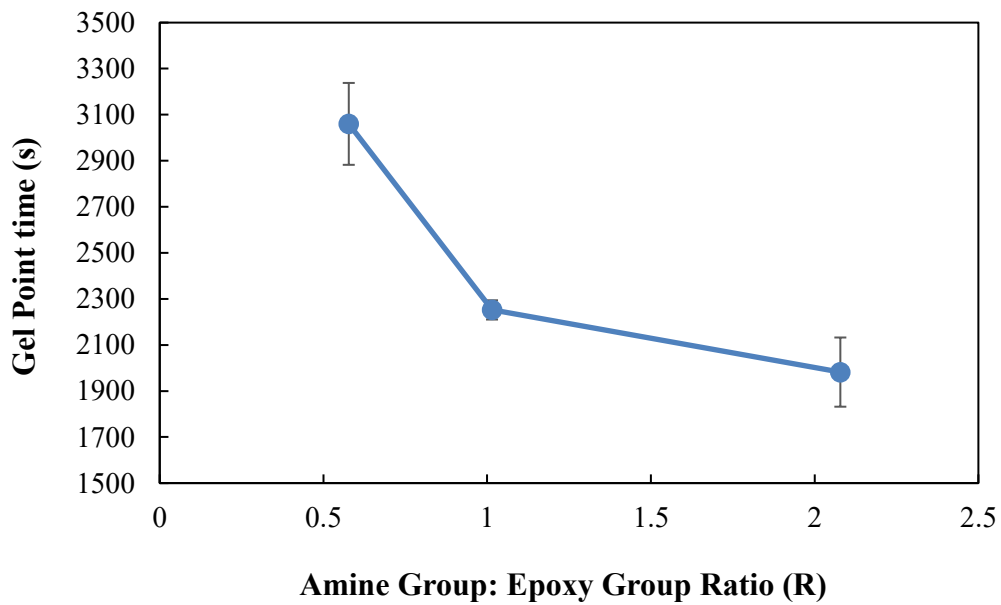


Figure 14. Plot of gel point versus R value.

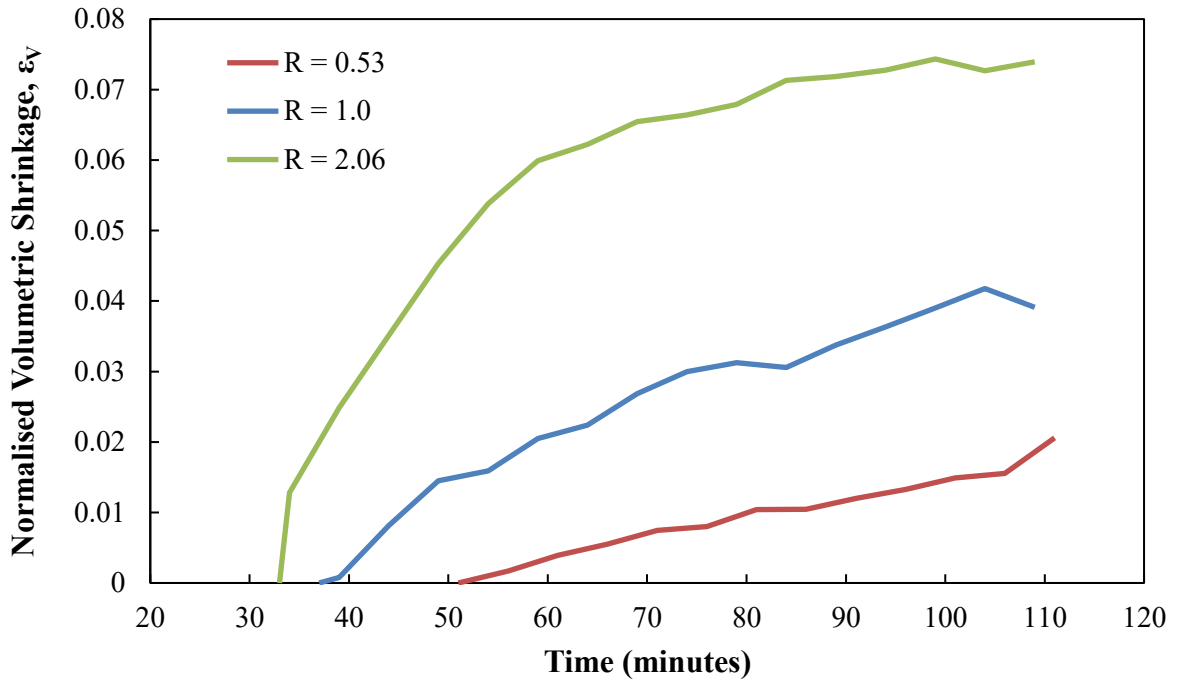


Figure 15. Adjusted cure shrinkage results measured using hot-stage microscopy taking account for gel point.

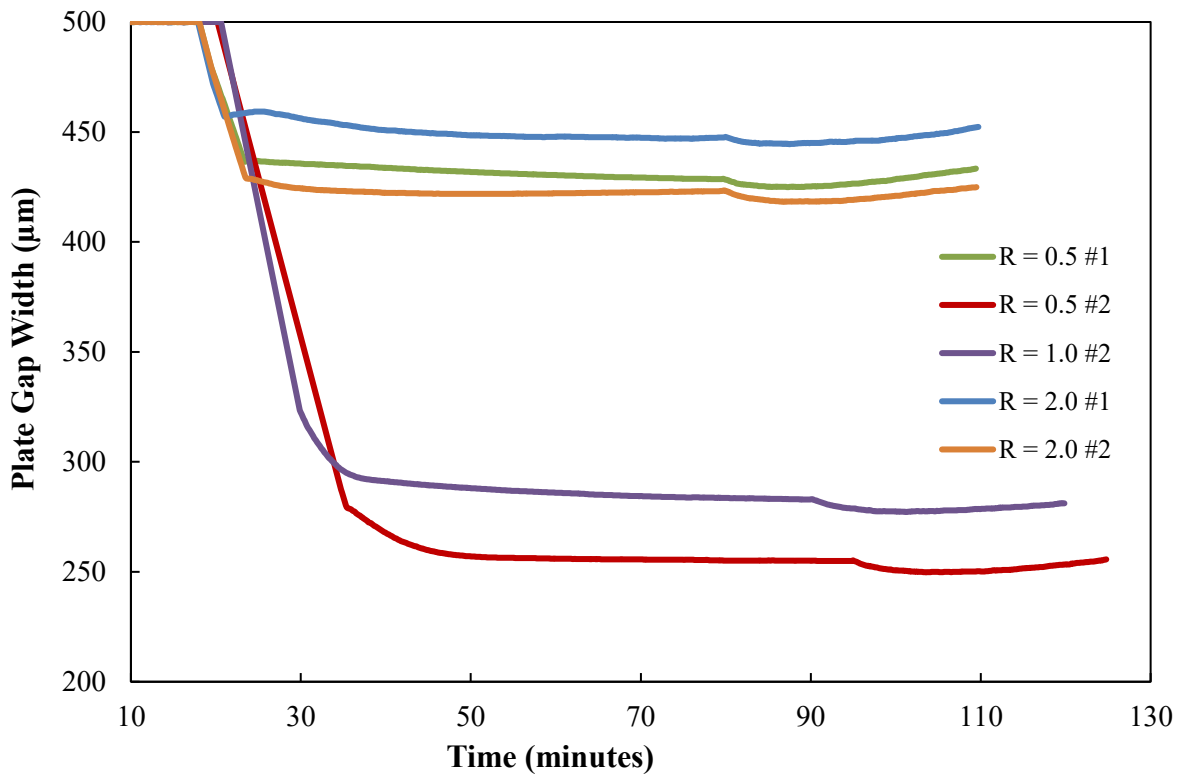


Figure 16. Plot of rheometer plate gap width versus time into curing schedule.

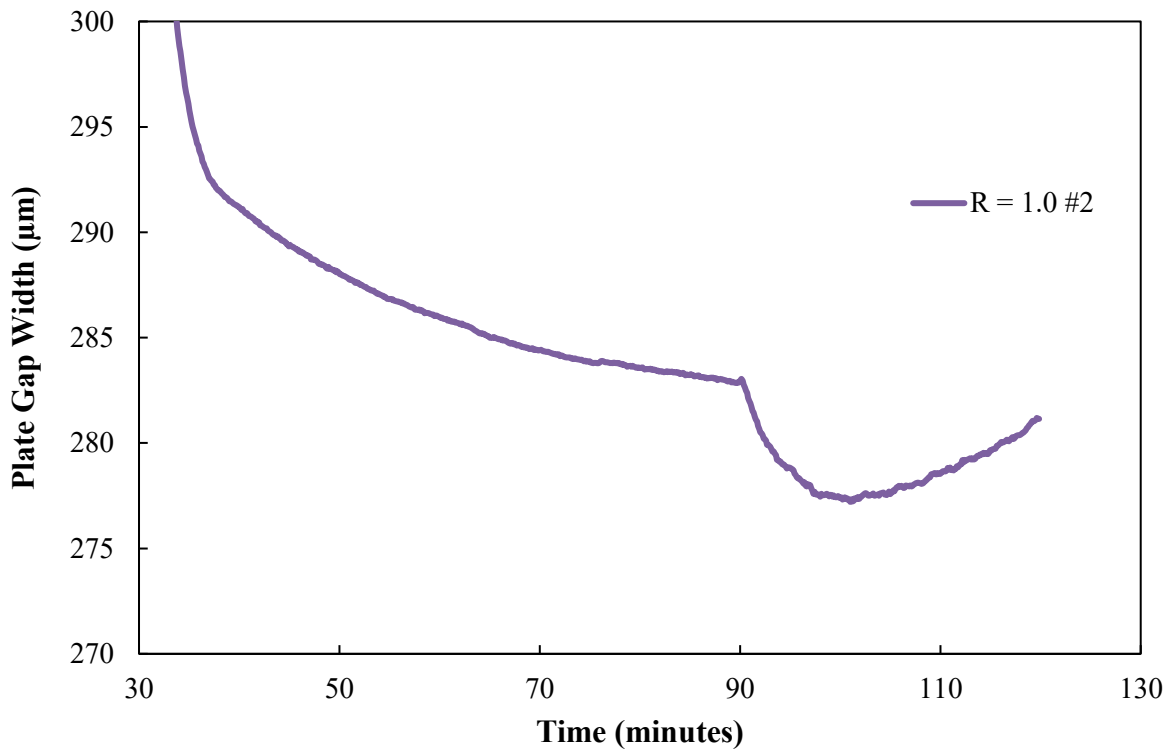


Figure 17. Magnified plot of rheometer plate gap width versus time into curing schedule for sample number 2 with a R ratio of 1.0.

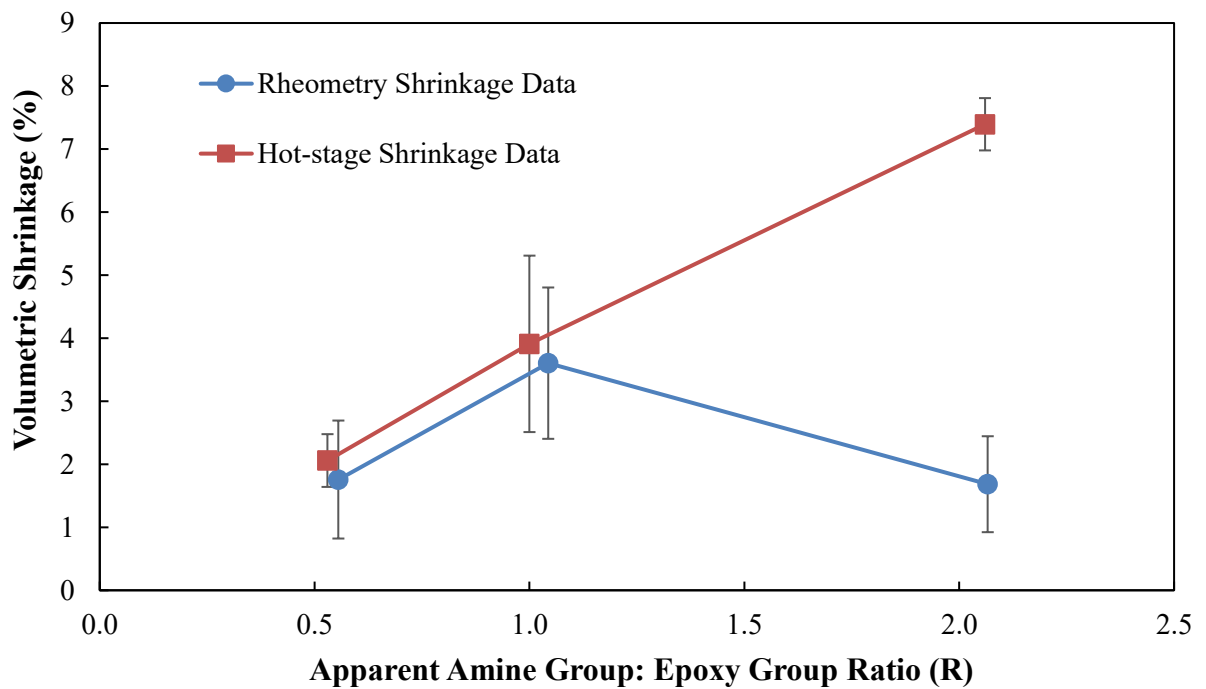


Figure 18. Comparison of cure shrinkage results measured using the rheometer and hot-stage techniques.